Chapter 11
A Novel Method to Quantify Fugitive Dust Emissions Using Optical Remote Sensing

Ravi M. Varma[1,*], Ram A. Hashmonay[1], Ke Du[2], Mark J. Rood[2], Byung J. Kim[3], and Michael R. Kemme[3]

Abstract This paper describes a new method for retrieving path-averaged mass concentrations from multi-spectral light extinction measured by optical remote sensing (ORS) instruments. The light extinction measurements as a function of wavelength were used in conjunction with an iterative inverse-Mie algorithm to retrieve path-averaged particulate matter (PM) mass distribution. Conventional mass concentration measurements in a controlled release experiment were used to calibrate the ORS method. A backscattering micro pulse lidar (MPL) was used to obtain the horizontal extent of the plume along MPL's line of sight. This method was used to measure concentrations and mass emission rates of PM with diameters ≤10 μm (PM_{10}) and PM with diameters ≤2.5 μm ($PM_{2.5}$) that were caused by dust from an artillery back blast event at a location in a desert region of the southwestern United States of America.

Keywords: Fugitive dust, emission estimation, optical remote sensing, particulate matter, PM_{10}, $PM_{2.5}$, Mie theory, FTIR, transmissometer, micro pulse lidar

11.1 Introduction

Particulate matter (PM) emissions from fugitive sources are a major concern because of their contribution to degradation of air quality. Several studies in the past have shown that PM with diameters ≤10 μm (PM_{10}) and PM with diameters

[1] *ARCADIS, 4915 Prospectus Drive Suite F, Durham, NC 27713, USA*

[2] *Department of Civil & Environmental Engineering, University of Illinois at Urbana-Champaign, 205 N. Mathews Ave., Urbana, IL 61801, USA*

[3] *U.S. Army ERDC—CERL, 2902 Farber Drive, Champaign, IL 61822 USA*

**Current affiliation: Department of Physics, National University of Ireland, University College Cork, Cork, Ireland; Tel: +353-21-4903294, Fax: +353-21- 4276949*

Y.J. Kim and U. Platt (eds.), *Advanced Environmental Monitoring*, 143–154.

≤2.5 μm ($PM_{2.5}$) have adverse effects on human health in the areas surrounding these sources. This paper presents a method for quantifying fugitive dust emissions using optical remote sensing (ORS) techniques. The method makes use of path-integrated multi-spectral light extinction measurements in a vertical plane by ORS instruments downwind of a fugitive PM source. The light extinction measurements are used to retrieve path-averaged $PM_{2.5}$ and PM_{10} mass concentrations using inversion of the Mie extinction efficiency matrix for a range of size parameters. This retrieval needs to be calibrated against a standard mass concentration measurement for the specific dust of interest. This novel method was applied for dust plumes generated by artillery back blast in a desert area of the southwestern United States of America (USA).

The ORS instruments used for mass concentration retrieval in this study include two monostatic active open path-Fourier transform infrared spectrometers (OP-FTIRs) and two open path-visible laser transmissometers (OP-LTs). In addition to the above ORS instruments, a backscattering micro pulse lidar (MPL, Sigma Space Corporation, Maryland, USA) was also used to obtain the horizontal extent of the PM plume along the MPL's line of sight. In this study, the mass concentration retrieval part of the ORS method was calibrated using concurrent measurements by DUSTTRAK (DT) aerosol monitors (Model 8520, TSI, Inc., Minnesota, USA) in the corresponding particle size ranges that were traced back to particulate mass filter calibrations. Once the mass concentrations were retrieved from each set of ORS instruments in a vertical plane of measurement, the emission rates across the plane were computed by fitting a bivariate Gaussian function to the data (Hashmonay et al. 2001). The ORS method was applied for PM mass emission quantification due to an artillery back blast.

11.2 Method

The ORS method to retrieve PM mass concentrations relies on multi-spectral path-integrated light extinction measurements. Light extinction (absorption + scattering) as a function of wavelength can be computed by Mie theory if the optical properties and the size distribution of the PM are known. The optical properties are expressed in terms of the complex refractive index, m, and are defined as (Kerker 1969):

$$m = n - in\kappa \tag{1}$$

where the real part of the refractive index, n, is defined as the ratio between the wavelength of light in free space, λ_0, and the wavelength in matter, λ. The imaginary part of the complex refractive index, $n\kappa$, is the absorption factor, and the absorption index (κ) is related to the absorption coefficient of the matter. If the PM is non-absorbing, then the light extinction is due to scattering alone and the refractive index will have a non-zero real part and a zero imaginary part. In such a scenario, the real part of the refractive index is nearly constant for a wide range of non-absorbing wavelengths.

The extinction efficiency is a function of the particle diameter, d, and λ and m. When a broad spectral band of incident light is detected, the extinction efficiency for each combination of particle sizes and wavelengths need to be calculated. Our method for calculating the Mie extinction efficiencies follows the recurrence procedure in Wickramasinghe (1973). These extinction efficiency values are organized in a matrix, $Q_{e\,ij}$, where each row (i) is for a different λ and each column (j) is for a different particle size range. The matrix, $Q_{e\,ij}$, is calculated by using a predetermined constant refractive index for the relevant spectral range (which is corrected by a calibration procedure) and for particle diameters up to 20 μm. The extinction coefficient, σ_e, is expressed in cm^{-1} as a function of wavelength and for a given size distribution as (Hashmonay and Yost 1999):

$$\sigma_{e_i} = \frac{\pi}{4} \sum_j Q_{e_{ij}} N_j d_j^2 \tag{2}$$

where N_j is the particle number density at the j^{th} particle size class in cm^{-3} and d_j is the mean particle diameter of the j^{th} particle size range in centimeter. The value of N_j is the unknown that needs to be calculated by the inversion method. The ORS measurements provide the extinction spectra (σ_{ei} in Eq. 2) that is an input to the iterative inversion algorithm. The kernel matrix for the inversion procedure is $Q_{e\,ij}$, which includes the extinction efficiency values for a range of wavelengths and particle sizes. We use a multiplicative relaxation algorithm for the inversion procedure (Chahine 1970), which was originally developed for radiative transfer applications. There is no need to pre-define a particle size distribution and the algorithm iteratively converges to the unique best fit regardless of the first guess. Multiplying the resulting particle size distribution by its corresponding size bins' mean diameter cubed and particle density provides the mass distribution.

To illustrate the inversion, we use a typical ORS dust extinction spectrum collected using one OP-FTIR and one OP-LT with collinear optical paths. This experiment investigated the optical extinction properties of dust samples collected from an artillery back blast site at a desert location in the southwestern USA. A centrifugal blower released the dried and sifted dust approximately normal to the beam paths in a controlled manner. During this simulation, 1-s data were acquired using the OP-LT (at 0.67 μm) and 4-s data were acquired using the OP-FTIR (2–13.5 μm spectral range) at 4 cm^{-1} resolution. The baseline of absorbance (optical depth) spectra was flat at zero when no dust was encountered by the light except for the absorption bands for H_2O vapor and CO_2 (spectral bands around 2.5 μm, 4.2 μm, and from 5.5 to 7 μm). These absorption bands in the infrared wavelengths show up in the spectra with or without dust encountered in the ORS beam path. The spectrum (open diamonds) shown in Fig. 11.1 is an example with dust encountering the light beam from the OP-FTIR and OP-LT. The OP-LT extinction at 0.67 μm is shown as the far left data point in the spectrum, and is averaged over the time period of the OP-FTIR data acquisition. The broad absorption feature of the back blast dust at around 10 μm is much stronger when compared to other dust samples studied by the authors. The sharp singularity-like feature between 11.2 and 11.6 μm is similar to other previously sampled dusts. These two unique features together enable us to identify the

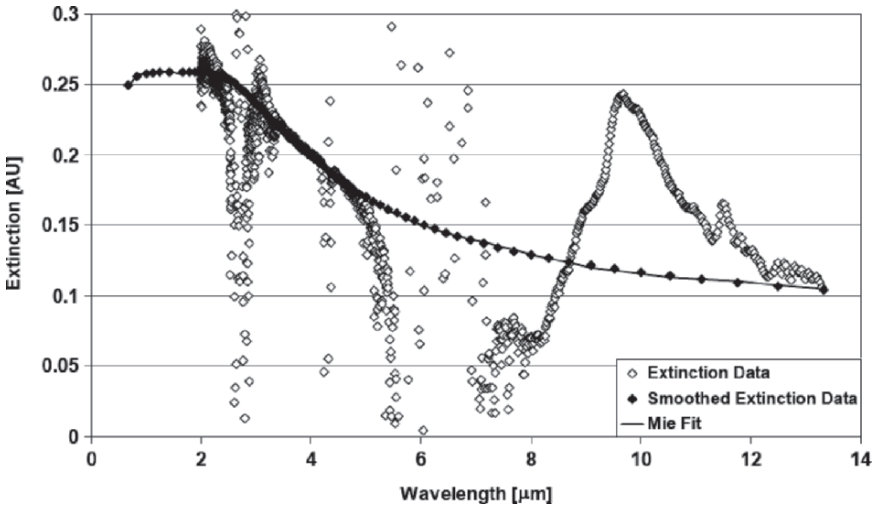

Fig. 11.1 Multi-spectral light extinction spectra by ORS instruments (OP-FTIR and OP-LT)

suspended dust that is generated by the artillery back blast during the field campaign in the southwestern USA.

Seven wavelengths were chosen from the OP-FTIR spectrum that avoid unique dust features and other gaseous absorption peaks so that the light extinction values at each wavelength are due to scattering alone. The wavelengths used to obtain the extinction values for the smoothed extinction distribution are 2.4, 3.5, 3.8, 4.1, 4.4, 4.9, and 13.2 μm (in addition to the OP-LT wavelength of 0.67 μm). A triangle-based cubic interpolation was performed between those wavelengths to generate 90 interpolated data points that were used to compute the extinction efficiency (kernel) matrix ($Q_{e_{ij}}$). The interpolated data set enhances the over-determination of the inversion problem and ensures a unique solution. The resulting interpolated extinction values define the baseline offset (when dust is encountered by light) that excludes the extinction caused by H_2O vapor and CO_2 and avoids other gaseous and PM absorption features. These interpolated extinction values are shown in the Fig. 11.1 as solid diamonds. Also, we used 54 bins that describe particle diameters ranging from 0.25 to 20 μm on a log scale. The first 43 bins that correspond to PM_{10} are of interest for this study. For illustration, we assumed an initial complex refractive index (1.6, 0) which is representative of airborne dust from the desert (Grams et al. 1974) for a range of non-absorbing wavelengths. To achieve proper apportionment of PM_{10} and $PM_{2.5}$ in the retrieved mass distributions, a correction was made to this value as explained in the calibration section below. After the matrix was computed, we inverted it to get number concentrations for all the 54 diameter bins (mid-point of each diameter range in the log scale). The retrieved size (mass) distribution up to 10 μm, which is of importance to characterize PM_{10}, is shown in Fig. 11.2. Mie calculations were then completed in the forward direction to see if the retrieved extinction spectrum from the derived size distribution fit well with the input extinction data (solid line in Fig. 11.1). $PM_{2.5}$ concentration can

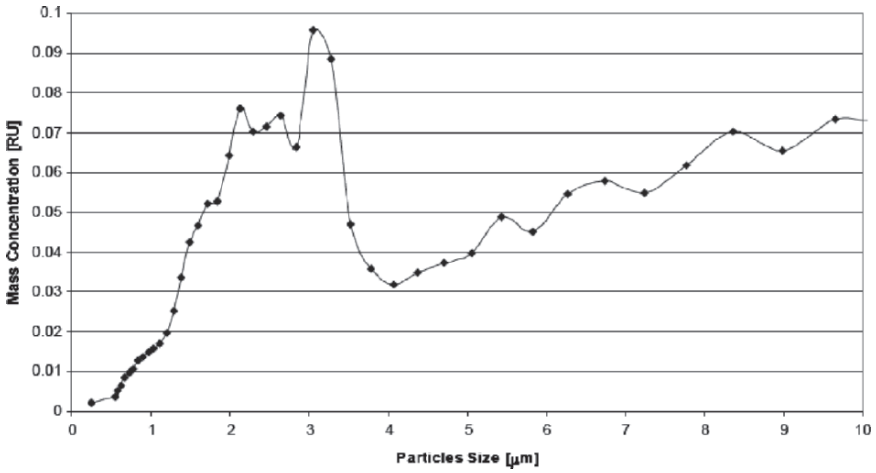

Fig. 11.2 Mass distribution retrieved from multi-spectral ORS measurement. RU = relative mass units

then be calculated by adding the mass concentrations in all particle size bins up to 2.5 μm, and PM_{10} concentration can be calculated by adding the mass concentrations in all particle size bins up to 10 μm.

11.3 Calibration of ORS Method

Calibration of the ORS method was done with a two-step approach by comparing $PM_{2.5}$ and PM_{10} mass concentration values retrieved by the ORS method to $PM_{2.5}$ and PM_{10} measured mass concentration values that were obtained by a pair of calibrated DT aerosol monitors. The DT monitors measure particle mass concentration of PM_{10} or $PM_{2.5}$ when using the corresponding inlet attachment. The first step in the ORS calibration is to retrieve the right apportionment of $PM_{2.5}$ and PM_{10} in the dust plume and the second step is to get the right mass concentration value for both $PM_{2.5}$ and PM_{10}. An experiment was performed with a controlled release of dust from the artillery back blast site in a tent with a 3-m beam path. The tent was used to enclose the optical path of the ORS to avoid influence from ambient wind, and to ensure as uniform a dust plume as possible throughout its beam path. The monostatic OP-FTIR and the OP-LT were placed close to each other so that the combined optical beams formed the ORS optical beam path for the experiment. The dust plume was generated and introduced into the ORS beam path using a blower to entrain the dust and a fan to disperse the dust uniformly in the beam path. Two DT aerosol monitors were placed inside the tent mid-way along the ORS beam path, with one DT using a $PM_{2.5}$ inlet attachment and the other using a PM_{10} inlet attachment. The ORS and DT measurements were temporally synchronized and each data point for comparison is an average of 10 s. The $PM_{2.5}$ and PM_{10} mass

concentrations were retrieved from ORS extinction measurements, as explained in the previous section. The $PM_{2.5}$ and PM_{10} data collected by the DT aerosol samplers were averaged for the same period as the ORS data. The DT samplers were previously calibrated against filter-based mass concentration measurements at the artillery facility (and prior to this experiment) for $PM_{2.5}$ and PM_{10}.

The ORS-retrieved PM_{10} data were plotted against the corrected PM_{10} from the DT samplers with the PM_{10} inlet attachment, and the ORS retrieved $PM_{2.5}$ data were plotted against the corrected $PM_{2.5}$ from the corresponding DT sampler. The slopes of both scatter plots were different, which means that the ORS method needs to be corrected to obtain the right apportionment of $PM_{2.5}$ and PM_{10} in the dust plume. The goal was to complete the ORS mass concentration retrieval algorithm to obtain the correct PM_{10} and $PM_{2.5}$ apportionment in the dust plume (as seen by the DT aerosol samplers), while using only one calibration factor (named apportionment factor). This goal was achieved by iteratively changing the apportionment factor that multiplies the initially assumed refractive index of 1.6, re-computing $Q_{e_{ij}}$, and then inverting the matrix to retrieve the mass distribution. This process was repeated until the slopes of both the PM_{10} and $PM_{2.5}$ scatter plots were nearly the same. Factorizing the real part of the complex refractive index adjusted the apportionment to be traceable to the mass filters' apportionment. A factor of 0.86 (equivalent to a refractive index of 1.37) provided the most accurate apportionment for about 70 dust plume measurements during the calibration experiments, and was used in the inversion method for the entire dataset that was collected from the artillery back blast site. The evolution of retrieved mass distribution for one of the extinction spectra measured at the artillery site is shown in Fig. 11.3 for three refractive index values. It is apparent

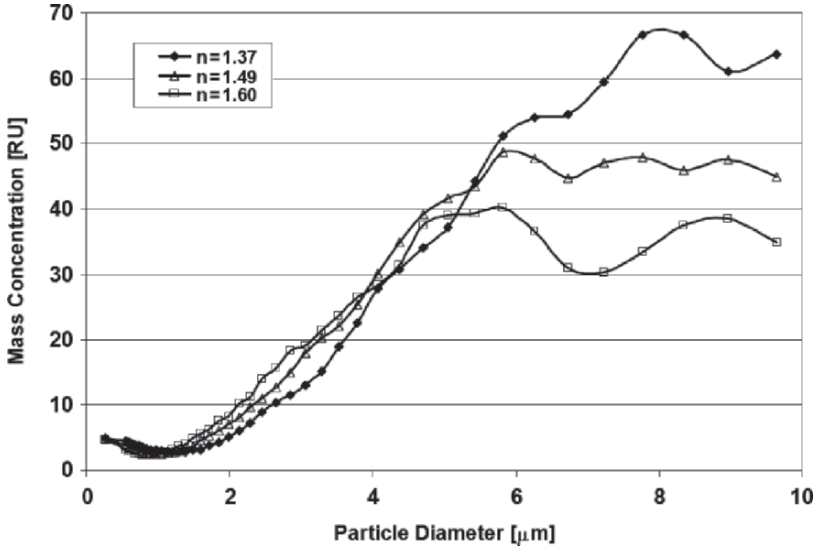

Fig. 11.3 Dependence of mass distribution on refractive index. n = refractive index, RU = relative mass units

that changing the refractive index values in the ORS method calibration effectively changes the retrieved apportionment of $PM_{2.5}$ and PM_{10} in the dust plume.

Once the right apportionment is achieved, then a common multiplicative factor is used to get the correct PM_{10} and $PM_{2.5}$ mass concentrations. This multiplicative factor (named mass factor) is to make the slope of the ORS mass concentrations scatter plot against the DT aerosol sampler derived mass concentrations to 1. The above two calibration factors (apportionment and mass) will be different for different kinds of dust samples and the calibration procedure needs to be performed on a case to case basis. The calibration scatter plots for the artillery back blast dust are as shown for PM_{10} and $PM_{2.5}$ in Fig. 11.4a and b, respectively. The R^2 values from the comparison are 0.78 for PM_{10} and 0.72 for $PM_{2.5}$. These excellent correlations between the open path and point measurements were obtained despite the fact that the pair of DT samplers and ORS instruments had imperfect synchronization of the temporal and spatial measurements. After the calibration, the data from the artillery back blast field campaign were corrected for the ORS mass concentration retrieval.

The first step of the calibration procedure to obtain the apportionment factor reduces the uncertainty from assuming optical properties of the PM material (i.e., real part of refractive index). Both steps of the calibration rely on accurate and concurrent $PM_{2.5}$ and PM_{10} measurements using a standard method (e.g., calibrated DT aerosol monitor).

11.4 Application of ORS Method for PM Emission Rate Estimation

The ORS method to retrieve aerosol mass concentrations was applied to measure $PM_{2.5}$ and PM_{10} mass emission rates from artillery back blast at a desert location in the southwestern USA during October 27, 2005. Tests were carried out on improved gun placements (i.e., artillery were located on surfaces that had been modified to enhance ease of firing and potentially mitigate dust emissions). The extinction spectra of soil dust and canon smoke were separated from each other as a result of field tests that occurred at the artillery site when it rained on one day of the test. The rain moistened the soil and caused the artillery back blast plume to contain only soot associated with the discharge of the propellant, but no dust. From our past experience with black carbon extinction spectra (graphite and black smoke), and from this day of measurements we confirmed that the soot particles had a flat, constant extinction value across visible and infrared wavelengths (due to absorption). During our calibration experiments, with the dust collected from an artillery site, we observed a constant ratio between the peak value at 10 μm (0.24 in Fig. 11.1) and the minimum value at 8 μm (0.07 in Fig. 11.1). This ratio for pure dust from this site was 3.4 (= 0.24/0.07). Therefore, the contribution from soot particles in the mass emission rate calculations were separated from that of the dust particles by subtracting a constant value of extinction throughout the spectrum (calculated by

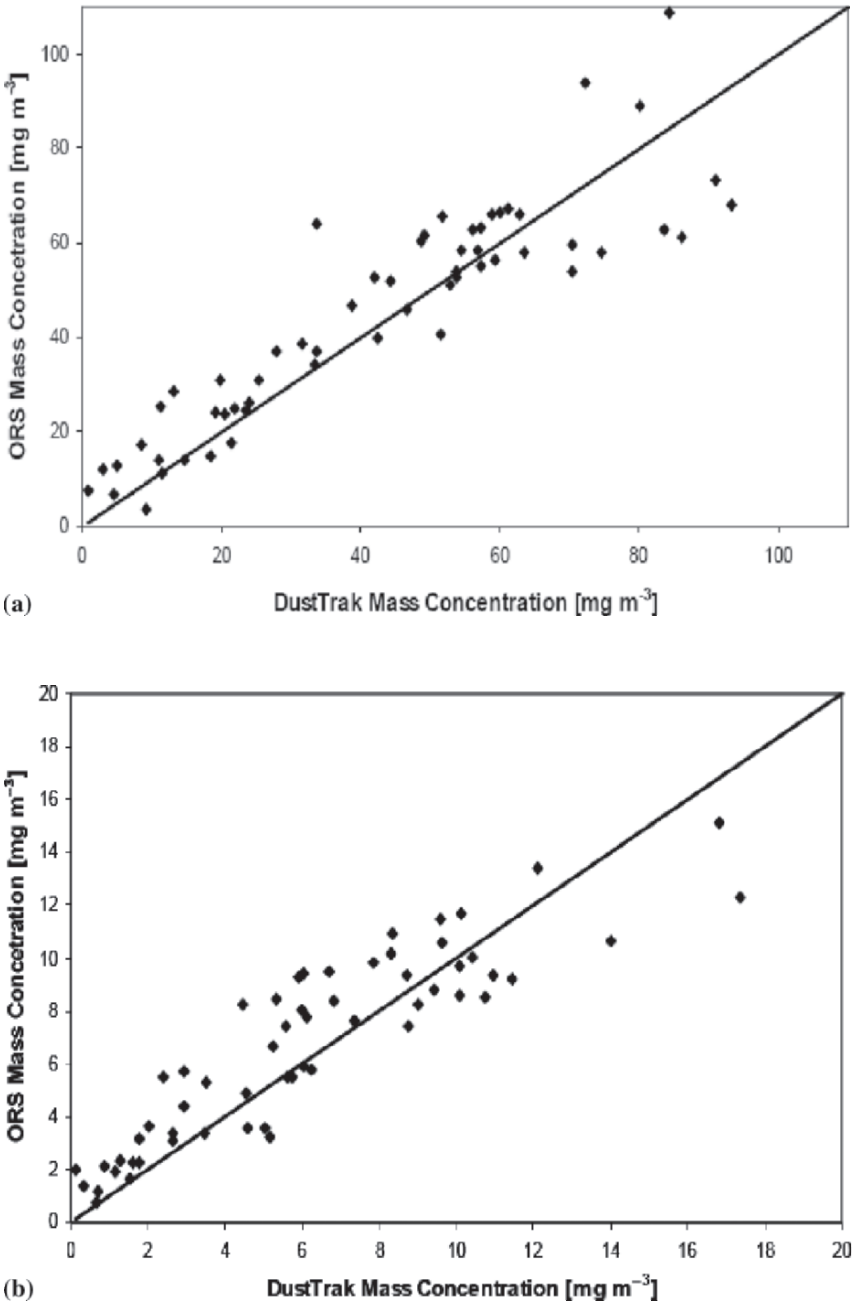

Fig. 11.4 **a** PM_{10} calibration curve ($y = 1.00x$, $R^2 = 0.78$). **b** $PM_{2.5}$ calibration curve ($y = 1.00x$, $R^2 = 0.72$)

solving a simple algebraic equation), thereby maintaining the known ratio between the values at the maximum to the minimum of the dust absorption feature.

An example of the application of the ORS method to quantify PM mass emission is explained below. A full presentation and discussion of the data are beyond the scope of this paper. We used two pairs of OP-FTIR/OP-LT ORS instruments to measure mass concentrations of PM across the plumes that were generated by artillery back blast events (Fig. 11.5). Both pairs of ORS instruments were located next to each other and their beams crossed at about 30 m downwind of the artillery gun location. The first ORS beam path was close and parallel to the ground, and directed toward a retroreflector that was placed at the bottom of a tower (scissor lift) and 100 m away from the location of the first pair of OP-FTIR/OP-LT (hereafter, ORS lower beam path). The second ORS beam path was elevated in such a way that the OP-FTIR/OP-LT pair was looking at a retroreflector placed 15 m above the ground on the same tower as the retroreflector that was at the ground level (hereafter, ORS upper beam path). The dust plume generated from the back blast was brought to the vertical measurement plane of the ORS by a predominantly southwesterly wind. The MPL was another ORS instrument used in this field campaign (Du et al. 2006), which was placed along the same path of the other ORS systems, but was located behind their location by 410 m. Backscatter data from the MPL were used to determine the horizontal profile of plumes along the ORS line of sight (shown inside the box in Fig. 11.5).

Intermittent artillery firing took place between 11:35 AM and 3:30 PM on October 27, 2005. Both OP-FTIRs (the lower one looking at the ground-level retroreflector and the elevated one looking at the elevated retroreflector) collected roughly 10-s spectra at 0.5 cm^{-1} resolution, and were averaged over the duration of

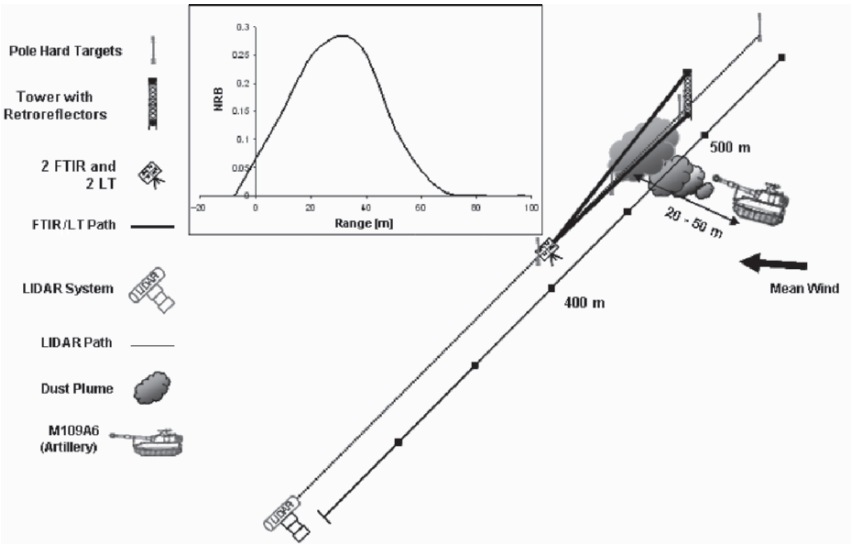

Fig. 11.5 Setup on October 27, 2005, at an artillery facility in southwestern USA. MPL backscattered intensity profile is shown in the box along ORS lower beam path

each plume event (corresponding to each shot). Data collected from each OP-LT were averaged for the same time-interval as the corresponding OP-FTIR. The combined spectra for each plume event were used in conjunction with an inversion algorithm to retrieve $PM_{2.5}$ and PM_{10} mass along each beam path. The following calculations were made for one plume from an artillery firing event, identified as number 172 during the field campaign. The baseline extinction values, averaged for this plume event from the ORS lower beam path and the ORS upper beam path, are shown in Table 11.1. These points are representative of the baseline features of the ORS optical depth spectrum by excluding the gaseous as well as PM absorption features, as explained in the ORS method for the mass concentration retrieval procedure discussed before. We used the calibrated ORS method to compute $PM_{2.5}$ and PM_{10} mass concentrations along the ORS lower and upper beam paths. From the retrieved mass concentrations, $PM_{2.5}$ and PM_{10} were calculated for both the ORS lower and upper beam paths (Table 11.2). The differences in path-integrated mass concentrations between the lower and upper beam paths provide vertical dilution information of PM mass.

The vertical extent of each plume can be calculated from the plume dilution information obtained from the two pairs of OP-FTIR/OP-LT beam paths. Following a previous study (Hashmonay et al. 2001) we fitted a bivariate Gaussian function to the ORS data. This method, which is also called the radial plume mapping method, is being used for gas pollutant emission rate quantification, and is also applicable for quantifying PM mass emission rate. For estimating the emission rate by Hashmonay

Table 11.1 Extinction values used from ORS spectrum for mass retrieval

Wavelength (μm)	Lower ORS beam path	Upper ORS beam path
0.67	0.194	0.100
2.4	0.235	0.078
3.5	0.254	0.067
3.8	0.236	0.062
4.1	0.221	0.061
4.4	0.213	0.058
4.9	0.201	0.055
13.2	0.130	0.040

Table 11.2 Path-averaged PM mass in ORS beam paths

	$PM_{2.5}$ mass concentration (mg m^{-3})	PM_{10} mass concentration (mg m^{-3})
Upper ORS beam path	0.36	1.2
Lower ORS beam path	0.42	4.1

et al. (2001), the parameters of the assumed Gaussian function were iteratively calculated from the path-integrated OP-FTIR gas absorption measurements from five retroreflectors in the vertical measurement plane used in that study. These parameters are the normalization coefficient, peak location on the ground along the OP-FTIR line of sight, and the horizontal and vertical standard deviations of the Gaussian plume profile. In this study, we used the vertical dilution information from mass concentrations to obtain the vertical standard deviation of the plume profile. Instead of several retroreflectors placed on the ground (as in the case of Hashmonay et al. 2001), we used the MPL to obtain horizontal peak location as well as the horizontal standard deviation for the Gaussian plume function. The MPL was operated in the field, aligned collinear to the ORS lower beam path and across the plume, to get the plume dimension along its line of sight. The MPL profile that was averaged for this plume event is shown inside the box in Fig. 11.5. The *x*-axis of this plot is along the ORS lower beam path. The origin of this plot is fixed at the OP-FTIR/OP-LT pair location (not the MPL). From this plume profile along the ORS lower beam path, we assessed the peak location at 35 m from origin with a standard deviation of 19 m. We fixed the vertical plume peak location on the ground.

Once the mass-equivalent plume profile was obtained, we integrated the mass concentration over the entire plane of measurement (both for $PM_{2.5}$ and PM_{10} separately). These plane-integrated mass concentrations (in units of g m^{-1}), in conjunction with the wind vector normal to the plane (in m s^{-1}) provided the mass emission rate of dust generated from the artillery back blast (in g s^{-1}). Fig. 11.6 shows the reconstructed mass-equivalent plume profile in the vertical plane of measurement for this back blast event of roughly 20-s duration. The upper ORS beam path and the tower with retroreflectors are also shown, for reference, as dark vertical bars at a crosswind distance of 100 m. An average wind speed of 4.5 m s^{-1} and a wind direction of 17° normal to the plane of measurement were measured for the duration of the entire event. This wind vector and the reconstructed PM mass concentration profile (for both $PM_{2.5}$ and PM_{10}) integrated over the plane of measurements were

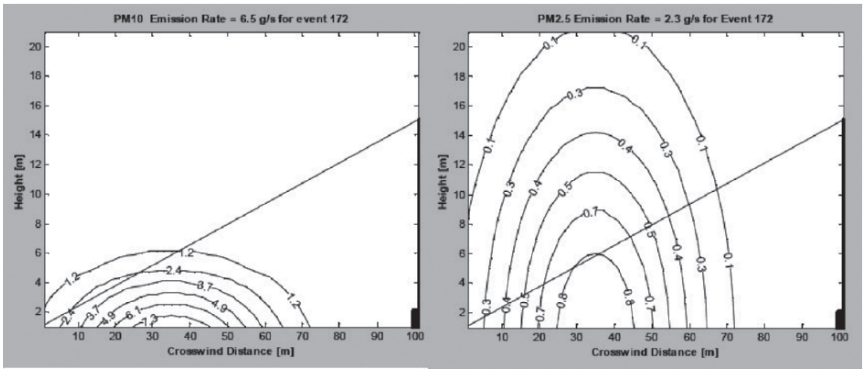

Fig. 11.6 Reconstructed PM_{10} and $PM_{2.5}$ mass-equivalent plume profiles. The contour values are in mg m^{-3}

used to compute the emission rate of PM mass across the plane of measurements. The PM_{10} mass emission rate for this event was calculated as 6.5 g s^{-1} and the $PM_{2.5}$ mass emission rate was calculated as 2.3 g s^{-1}. The total amount of PM_{10} and $PM_{2.5}$ generated for the duration of this plume was 130 and 46 g, respectively.

11.5 Summary

A new and innovative optical remote sensing (ORS) method was described here to obtain particulate matter (PM) concentrations and mass emission rates that are generated by fugitive dust events. Multi-spectral path-integrated measurements were used as part of the ORS system. This method was successfully calibrated by determining calibration factors using concurrent conventional mass concentration measurements in a closed chamber with controlled dust plume releases. Field measurements were carried out at a southwestern USA desert location where dust plumes were generated from the shock of artillery back blast. We developed a simple method for eliminating the error in dust mass emission rate estimations introduced by soot particles from the cannon by maintaining the ratio of maximum to minimum extinction values around a prominent dust absorption feature in the spectrum, as estimated during calibration experiments. The horizontal extent of the plumes along the ORS line of sight were obtained by backscatter measurements from a micro pulse lidar. PM with diameters ≤10 μm (PM_{10}) and PM with diameters ≤2.5 μm ($PM_{2.5}$) mass emission rates and concentrations were obtained by making multiple ORS measurements on a vertical plane downwind of the PM source in conjunction with the wind vector.

Acknowledgements The authors like to thank Dr. Jack Gillies and Dr. Hampden Kuhns, Desert Research Institute (DRI) for providing the DUSTTRAK calibration data against DRI filter-based measurements made during our combined field measurements. This research was sponsored by the Strategic Environmental Research and Development Program grant number CP-1400.

References

Chahine M.T. (1970), Inverse problems in radiative transfer: Determination of atmospheric parameters, *J. Atmos. Sci*., 17, 960–967.

Du K., Rood M., Kim B., Kemme M., Hashmonay R., and Varma R. (2006, June), Optical Remote Sensing of Dust Plumes Using Micropulse Lidar, (Paper presented at the 99th Annual Meeting of the Air & Waste Management Association, New Orleans, Louisiana, 315, 5 pp).

Grams G.W, Blifford Jr., I.H., Gillette D.A., and Russel P.B. (1974), Complex refractive index of airborne soil particles. *J. Appl. Meteor*., 13, 459–471.

Hashmonay R.A. and Yost M.G. (1999), On the application of OP-FTIR spectroscopy to measure aerosols: Observations of water droplets. *Environ. Sci. Technol*., 33(7), 1141–1144.

Hashmonay R.A., Natschke D.F., Wagoner K., Harris D.B., Thompson E.L., and Yost M.G. (2001), Field evaluation of a method for estimating gaseous fluxes from area sources using open-path Fourier transform infrared. *Environ. Sci. Technol*., 35, 2309–2313.

Kerker M. (1969), *The Scattering of Light*, (New York: Academic Press).

Wickramasinghe N.C. (1973), *Light Scattering Functions for Small Particles with Applications in Astronomy*, (London: Adam Hilger)